Phosphorylation of light-harvesting complex II controls excitation energy spillover between photosystems

Ryutaro Tokutsu[1,2†‡] *, Eunchul Kim[1†], Seiji Akimoto[3], Makio Yokono[1], Konomi Fujimura-Kamada[1], Norikazu Ohnishi[1], Yoshifumi Ueno[3], and Jun Minagawa[1,2]*

[1] Division of Environmental Photobiology, National Institute for Basic Biology, Nishigo-naka 38, Myodaiji, Okazaki 444-8585, Japan.

[2] Department of Basic Biology, School of Life Science, Graduate University for Advanced Studies, Okazaki 444-8585, Japan.

[3] Graduate School of Science, Kobe University, Kobe 657-8501, Japan.

[†] These authors contributed equally to this study.

[‡] Present address; Graduate School of Science, Kyoto University, Kitashirakawa Oiwake-cho, Sakyo-ku, Kyoto 606–8052, Japan.

* To whom correspondence should be sent. E-mail: tokutsu.ryutaro.4e@kyoto-u.ac.jp or minagawa@nibb.ac.jp

Abstract

Land plants and microalgae convert solar energy into electrochemical energy by using cooperative two photosystems (PSI and PSII). To maintain optimal photosynthetic rates under variable light conditions in nature, phosphorylation of light-harvesting complex for PSII (LHCII) balances the excitation energy distribution between the two photosystems. Here, we investigated the mechanism of this balancing in a green alga. We show that phospho-LHCIIs physically bind to both photosystems. The energy transfer from the LHCIIs to the PSII core complexes becomes less efficient, whereas the excitation level of PSI increases. The time-resolved fluorescence spectra showed an increase in delayed PSI fluorescence, which represents energetical spillover from PSII to PSI. In addition, the spillover is likely mediated by phospho-LHCIIs and PSI antennas. We hypothesize that the spillover explains the larger extent of phospho-LHCIIs dependent energy balancing in the green alga than land plants, which is important for the short-term photoadaptaion in the algal habitat.

Introduction

In photosynthesis, photosystem I (PSI) and photosystem II (PSII) in the chloroplast thylakoid membrane function in tandem and use light energy to drive redox processes. Under changing light conditions, the excitation levels of these photosystems are balanced to maintain an optimal photosynthetic rate. To this end, plants and green algae have an acclimation mechanism, called the state transition, which redistributes light-harvesting complex II (LHCII) between the two photosystems (1, 2). When PSII is preferentially excited (state 2-inducing conditions), the plastoquinone (PQ) pool gets reduced, which causes plastoquinol to bind to the cytochrome b_6f complex (Cyt b_6f). Cyt b_6f in turn activates a protein kinase (or kinases) required for LHCII phosphorylation (3). The phosphorylated LHCIIs (phospho-LHCIIs) migrate toward PSI to increase the absorption cross-section of PSI under state 2 conditions and thus balance photosystem excitation (4).

Several thylakoid-bound kinases have been reported, including the serine-threonine kinases STT7 and STL1 in *Chlamydomonas reinhardtii* (corresponding to STN7 and STN8 in *Arabidopsis thaliana*, respectively) and thylakoid associated kinase 1 (TAK1) in *Arabidopsis* (5). STT7 phosphorylates LHCIIs during state 1 to state 2 transitions and a mutant lacking STT7 was unable to phosphorylate LHCII under state 2-inducing conditions (6). Moreover, several reports indicated that STT7 interacts with subunit IV of Cyt b_6f in the stroma region (7). STT7 was activated (via physical modification (8)) when plastoquinol bound to the Qo pocket of the Cyt b_6f complex (9). Lemeille *et al.* revealed that STT7 activation requires a disulfide bridge between two cysteines at the N-terminus (10). The activated STT7 kinase is thought to directly phosphorylate LHCIIs.

Although many reports have described the roles of LHCII kinases in land plants and green algae, the molecular functions of phospho-LHCIIs during state 2 transitions are still under debate. Kyle *et al.* observed a significant amount of phospho-LHCIIs in the stroma lamellae of the thylakoid membranes, thus increasing the energy transfer between PSI and phospho-LHCIIs (11). Leister and coworkers suggested that phospho-LHCIIs were constantly associated with PSI in an Arabidopsis mutant lacking PsaE, a subunit of PSI (12). These reports agree with the model that phospho-LHCIIs migrate from appressed domains (grana, where PSII is enriched) to non-appressed domains (stroma lamellae, where PSI is enriched) of thylakoids during the state 2 transition, and thus, the phospho-LHCIIs connect to PSI (13). In contrast, Snyders and Kohorn observed significant amounts of LHCIIs in a roughly purified PSI-enriched fraction from a *tak1* mutant, indicating that LHCIIs could associate with PSI even when their phosphorylation was impaired, leading the authors to propose that LHCII phosphorylation was not essential for the lateral migration of LHCII toward PSI (5). Phospho-LHCIIs could associate with PSII in the absence of either the PSI-H or -L subunit in Arabidopsis (14). Tikkanen and colleagues also reported that LHCII phosphorylation was not a prerequisite for physical dissociation of the proteins from the PSII core, but instead contributed to the lateral migration of PSI-LHCII supercomplexes toward the grana margin (15, 16). While CP26, CP29 and LhcbM5 have been reported to bind to PSI during state 2 transitions in C. reinhardtii (Kargul et al. 2005, Takahashi et al. 2006, Drop et al. 2014), CP26 and CP29 are not found in the PSI-LHCI-LHCII supercomplex structure observed by Cryo-EM (Pan et al. 2021). Thus, it remains unclear whether phosphorylated LHCIIs shuttle from PSII to PSI.

Because the green alga *C. reinhardtii* has a large capacity for state transitions (17), the molecular functions of phospho-LHCIIs have been extensively investigated in this species. Iwai *et al.* observed that LHCIIs in PSII-LHCII supercomplexes were not phosphorylated, but those

2

75 that dissociated from PSII during the induction of state 2 were heavily phosphorylated, leading
76 the authors to hypothesize that phosphorylation is necessary for LHCIIs to undock from PSII
77 **(18)**. The undocked phospho-LHCIIs were shown to dissipate excitation energy, not only
78 increasing the absorption cross-section of PSI during state 1 to state 2 transitions **(19, 20)**. In
79 contrast, Wollman and colleagues reconfirmed that all phospho-LHCIIs that were detached from
80 PSII functionally bound to PSI without dissipating excitation energy, based on the
81 complementary changes in antenna sizes between PSII and PSI during state 1 to state 2
82 transitions observed by spectroscopic measurements **(17)**. Given the discrepancy over the
83 consequence of state transitions in *C. reinhardtii*, we performed comprehensive *in vivo* and *in*
84 *vitro* analyses to yield unambiguous insights into the functions of phospho-LHCIIs.

85   To elucidate the molecular functions of phospho-LHCIIs under state 2 conditions,
86 biochemical and spectroscopic analyses were conducted for cells and photosynthetic
87 supercomplexes stabilized by amphipol **(21)**. Biochemical approaches showed that the STT7-
88 dependent phosphorylation of LHCIIs was not a prerequisite for dissociation from PSII core
89 complexes. By time-resolved fluorescence spectroscopy, we also demonstrated that phospho-
90 LHCIIs altered the energy-transfer dynamics within the PSII-LHCII supercomplexes. Additionally,
91 the time-resolved fluorescence spectra showed an increase in delayed fluorescence from PSI in
92 state 2-induced cells, suggesting a novel function of phospho-LHCIIs whereby energy transfer
93 from PSII-LHCII to PSI-LHCI is stimulated via "spillover".

94

95 **Results**

96   *C. reinhardtii stt7* mutants such as *stt7-1* and *-2* **(6)** or *stt7-9* **(22)** are deficient in the
97 general kinase required for phosphorylation of LHCIIs and therefore can be used to investigate
98 the molecular functions of phospho-LHCIIs. In this study, we generated a single point mutation,
99 named *stt7-o*, via chemical-based random mutagenesis. The mutation in *stt7-o* causes a single
100 amino acid change from glycine to aspartic acid at amino acid 149 (supplemental Figure S1A),
101 which is internal of the kinase consensus domain of STT7. Although the *stt7-o* mutant
102 accumulated almost comparable amount of STT7 protein to WT (supplemental Figure S1B), this
103 mutant showed a severely deficient LHCII-phosphorylation phenotype under state 2 inducible
104 conditions (supplemental Figure S1C). These results indicate that the *stt7-o* mutant harbors
105 STT7 protein without its kinase function. We thus decided to use the *stt7-o* mutant as a mutant
106 deficient in LHCII phosphorylation.

107   To evaluate the state transition capability of the *stt7-o* mutant, we first observed
108 fluorescence-quenching kinetics under dark-anaerobic conditions where the state 1 to state 2
109 transition was induced **(17)**. As reported previously for the *stt7-1*, *-2*, and *-9* mutants, the *stt7-o*
110 mutant was deficient in state transition-dependent fluorescence quenching (qT), whereas the
111 wild-type (WT) strain showed a significant decrease in the maximum fluorescence yield under
112 dark-anaerobic conditions (Figure 1A, also see Figure S2 for fluorescence traces).

113   To estimate the amplitude of antenna dissociation from PSII during the state 2 transition,
114 we obtained single-turnover flash-saturation profiles of chlorophyll fluorescence to calculate the
115 relative functional absorption cross-sections of PSII. The measurements of the PSII antenna
116 absorption cross-section during state 1 to state 2 transitions showed a decrease in the maximum
117 fluorescence yield (~40%; Figure 1A), which is comparable to the level previously reported **(17)**.
118 Interestingly, it is inconsistent with the change of the relative PSII functional antenna size (~10%,

119 Figure 1B), implying that the LHCIIs were not functionally dissociated from the PSII core, but
120 quenched the excitation energy of PSII.

121 State transitions involve mechanisms that enable the two photosystems to balance their
122 excitation levels. To test this, we next performed fluorescence spectra analysis under low
123 temperature (77 K) to examine excitation energy re-distribution between the photosystems.
124 Upon functional association of LHCIIs with PSI under state 2 conditions, an increase in the
125 fluorescence peak could be observed at 713 nm because the fluorescence in the ranges of 670–
126 700 nm and 700–750 nm are attributable to PSII and PSI, respectively. The relative excitation
127 levels, shown as F713/F687 (i.e., the PSI/PSII emission ratio), increased during state 2
128 transitions (Figures 1C). These data, together with the phosphorylation kinetics of LHCIIs during
129 state 1 to state 2 transitions (Figure 1D), suggest that the LHCIIs were not functionally
130 dissociated from PSII, although they were phosphorylated and re-distributed energy from PSII to
131 PSI.

132 An inconsistency between the functional PSII antenna size and the fluorescence
133 quenching in state 2 implied that most phospho-LHCIIs were not physically detached from PSII,
134 even in WT cells. To further evaluate the fate of phospho-LHCIIs, we next performed sucrose
135 density gradient purification of the photosystems from state 2-locked thylakoid membranes. In
136 these membranes, LHCIIs were heavily phosphorylated (Figure S3), and showed quenching
137 capability as demonstrated by faster fluorescence decay compared to *stt7-o* thylakoids (Figure
138 S4). We obtained four different fractions from WT membranes, corresponding to free LHCII, PSI-
139 LHCI, PSI-LHCI/II, and PSII-LHCII supercomplexes from top to bottom of the tube (Figure 2A).
140 No PSI-LHCI/II band was observed in *stt7-o* thylakoids. As expected, the PSII-LHCII
141 supercomplex fraction appeared to be equally distributed in the state 2-induced membranes from
142 the WT and *stt7-o* strains.

143 The PSII-LHCII supercomplex fraction in the WT strain contained the same LHCII
144 composition as in the *stt7-o* mutant*,* as revealed by sodium dodecyl sulfate-polyacrylamide gel
145 electrophoresis (SDS-PAGE) analysis (Figure 2B), but the phosphorylation levels of LHCIIs were
146 clearly different (Figure 2C). Indeed, densitometric analysis of phospho-immunoblot images
147 revealed that at least four-fold heavier phosphorylation occurred in WT LHCIIs than in *stt7-o*
148 LHCIIs including CP26, CP29, and LHCII type I (Figure S5). The absorption spectra of those
149 PSII-LHCII fractions also showed superimposable shapes, even between 470 and 650 nm
150 (Figure 2D), which represents chlorophyll *b* absorption that is mainly coordinated in LHCIIs **(23,**
151 **24)**. These data suggested that the amount of LHCIIs associated with PSII was almost identical
152 in the PSII-LHCII supercomplexes obtained from the WT and *stt7-o* strains.

153 Steady-state fluorescence spectra of the PSII-LHCII supercomplexes at low-temperature
154 (77 K) showed negligible fluorescence from free LHCIIs (shoulder around 680 nm), even with the
155 preferential excitation of chlorophyll *b* (LHCII) at 480 nm (Figure S6). These results further
156 confirmed that the phospho-LHCIIs remained physically and tightly associated with the PSII core
157 complexes to absorb light energy, similarly in both strains under state 2 conditions. The increase
158 of fluorescence intensities in the ranges of 700–720 nm, which were only detected in PSII
159 complexed with phospho-LHCIIs (Figure S6; blue line, WT) implies the conformational changes
160 of LHCIIs as reported in higher plants **(25, 26)**. Because the PSII-LHCII supercomplexes were
161 not contaminated with PSI complexes as shown by SDS-PAGE analysis (Fig. 2B), it is plausible
162 that the increase of 700-720 nm fluorescence intensities implies modifications in the
163 conformation of the PSII-LHCII supercomplexes due to LHCII phosphorylation.

164   Fluorescence quenching analysis (Figure 1) showed that phosphorylated LHCIIs in PSII
165   (Figure 2) contributed to fluorescence quenching under state 2 conditions *in vivo*. To investigate
166   energy-transfer dynamics in PSII-LHCII supercomplexes with (WT) or without (*stt7-o*) phospho-
167   LHCIIs, we performed time-resolved fluorescence measurements followed by fluorescence
168   decay-associated spectra (FDAS) analysis (gray lines in Figures 3 and S7, Table S1). In the 1st
169   component of FDAS (~65 ps), we observed the energy transferred from LHCIIs to the PSII core
170   antenna CP43 as indicated by major positive peak around 680 nm (LHCII) and negative peak
171   around 685 nm (CP43). The red 700–720 nm component in the PSII-LHCII supercomplex of WT
172   was also observed, and was pronounced at the energy-trapping (~150 ps) and equilibration
173   states of the PSII core (~600 ps), indicating that the phospho-LHCII-dependent formation of a
174   low-energy state was coupled with PSII core complexes.

175   To qualitatively evaluate whether the altered excitation energy dynamics contributed to
176   excitation energy quenching, we performed up-conversion time-resolved fluorescence analysis
177   of the PSII-LHCII supercomplexes at room temperature. This analysis revealed only a little
178   quenching in the isolated PSII-LHCII supercomplexes (Figure S8), regardless of whether the
179   LHCIIs were phosphorylated. This result, together with the obvious fluorescence quenching in
180   both cell types (Figure 1A) and isolated thylakoids (Figure S4) in state 2, could indicate the
181   presence of a fluorescence quencher in the membrane that was not tightly associated with PSII
182   supercomplexes.

183   Based on these observations, the question arises as to why PSII-LHCII supercomplexes
184   alter the energy-transfer dynamics following LHCII phosphorylation. In other words, it is unclear
185   how phospho-LHCIIs in PSII-LHCII supercomplexes contribute to the excitation energy
186   redistribution between photosystems in state 2. The results obtained above implied that the
187   phospho-LHCIIs in the supercomplexes were involved in direct energy transfer from PSII-LHCII
188   to PSI-LHCI, which is traditionally termed "spillover". To verify the energy transfer occurring
189   between the membrane-embedded photosystems, we obtained 77 K time-resolved fluorescence
190   spectra of WT and *stt7-o* cells under both state 1 and state 2 conditions (Figure 3). After the
191   transition from state 1 to state 2, the PSI fluorescence (710–720 nm) in WT cells was enhanced
192   from the initial phase (0–49 ps) to 17 ns after excitation, representing an efficient redirection of
193   the energy to PSI, rather than PSII, whereas *stt7-o* mutant showed negligible change in this
194   fluorescence (Figure 3). This phenomenon corresponds to the re-association of LHCIIs with PSI
195   and the formation of PSI-LHCI-LHCII supercomplexes (Figure 2A), representing a conventional
196   state 2 transition.

197   We next analyzed the delayed fluorescence, which shows longer lifetime than intrinsic
198   relaxation of chlorophylls. Because delayed florescence with a time constant of ~20 ns at 77 K is
199   specifically derived from the charge recombination in the PSII reaction center **(27)**, the delayed
200   fluorescence spectrum reflects energy migration from the PSII core complexes. After the
201   transition from state 1 to state 2, the delayed fluorescence spectra in WT cells showed relatively
202   increased fluorescence in the PSI-fluorescence region (around 717 nm), whereas *stt7-o* cells
203   showed no obvious increase (red traces in Figure 4 and Table S2, WT and *stt7-o*). The
204   increased amplitude of the delayed fluorescence in the PSI-fluorescence region indicates that
205   the energy migrated from PSII core complexes to PSI under state 2 conditions.

206   This interesting change in the delayed fluorescence suggests that the transition from
207   state 1 to state 2 not only induced the migration of LHCII from PSII to PSI, but also facilitated
208   energy transfer from the PSII core to PSI. Indeed, the estimated ratio of spillover from the PSII-
209   PSI complex to total PSII, which was calculated as in a previous report **(28)**, increased two-fold

5

210 from 9.8% in state 1 to 19% in state 2 in WT cells. In addition, the results of a decomposition
211 fitting into the delayed fluorescence spectra clearly showed that the amplitudes of LHCII (679
212 nm) and PSII (CP43; 686 nm, CP47; 694 nm) decreased, whereas the amplitude of PSI (717
213 nm) and possibly phospho-LHCII and/or phospho-PSII (702 nm) increased in state 2-induced
214 WT cells (Figure 4 and Table S2). These results imply that phospho-LHCIIs under state 2
215 conditions induce energy transfer from PSII to PSI.

216   To investigate the energy interaction between PSII and PSI, we also analyzed the
217 delayed fluorescence in a mutant deficient in the PSI core (*ΔPSI*) (Figure S9). Although no
218 decrease in maximum fluorescence yield was observed during the state 1 to state 2 transition
219 (Figure S9A), state 2-inducible LHCII phosphorylation (Figure S9B) and changes in delayed
220 fluorescence spectra were observed in the *ΔPSI* strain (Figures 4 and Table S2). The delayed
221 fluorescence spectra showed a relatively large peak at 709 nm, which probably originated from
222 LHCI (magenta traces in Figure 4 and Table S2). These findings may represent an energy
223 transfer from the phosphorylated PSII-LHCII to free LHCI in the *ΔPSI* strain, implying that energy
224 transfer between photosystems was mediated by LHCI. Time-resolved fluorescence analysis of
225 purified PSII-LHCII supercomplexes obtained from WT and *stt7-o* strains under state 2
226 conditions showed almost identical spectra in delayed fluorescence (Figure 4), indicating that
227 energy was maintained in PSII-LHCII when PSI core and/or LHCI was absent. This further
228 supported the idea that the delayed florescence peak at 709 nm observed in *ΔPSI* mutant cells
229 were generated via spillover-dependent energy transfer from PSII-LHCII to LHCI. Collectively,
230 these results indicate that STT7-dependent LHCII phosphorylation regulates direct energy
231 interactions or "spillover" between PSII-LHCII and PSI-LHCI supercomplexes.

232

Discussion

234   State transitions have been recognized as energy balancing mechanisms mediated by
235 LHCII shuttling between photosystems. The phosphorylation of LHCIIs is a prerequisite for this
236 energy redistribution in thylakoid membranes. However, no reports have unambiguously
237 demonstrated the lateral migration of phosphorylated LHCIIs during state transitions. Here, we
238 present results showing that phosphorylated LHCIIs were not substantially dissociated from PSII
239 in a phosphorylation-dependent manner (Figure 2). However, the increased energy
240 accumulation in PSI was shown as an increased fluorescence ratio (F713/F687) in WT cells
241 (Figure 1). This result confirms the presence of phospho-LHCII-dependent excitation energy
242 redistribution between photosystems, which is widely accepted **(29)**. Time-resolved fluorescence
243 spectra analysis revealed that the redistribution of energy was coupled with energy transfer from
244 the PSII core to PSI-LHCI supercomplexes. These observations indicated that the molecular
245 mechanisms underlying the phospho-LHCII-dependent increase in PSI excitation involve
246 spillover from PSII to PSI.

247   It is difficult to distinguish between the phenomena of state transitions and spillover
248 because both mechanisms contribute similarly to energy redistribution between photosystems.
249 Indeed, many researchers have concluded that phospho-LHCII-dependent energy redistribution
250 reflected either state transitions or spillover (reviewed in **(13, 30)**). A consensus of the
251 mechanistic significance of STT7-dependent LHCII phosphorylation has not been reached thus
252 far. In this study, we focused on delayed fluorescence spectra (Figures 4 and S7) to evaluate
253 whether the STT7-dependent energy redistribution was mediated by the migration of phospho-
254 LHCIIs from PSII to PSI and/or via another mechanism involving phospho-LHCIIs. Delayed

6

255 fluorescence represents re-excitation of chlorophylls after charge recombination in the PSII
256 reaction center, where the fluorescence is not derived from other components, such as free
257 LHCII or PSI **(28)**. The delayed fluorescence observed in WT cells showed state 2-inducible
258 spillover from PSII-LHCII to PSI-LHCI, which was represented by strengthened delayed
259 fluorescence from 700–720 nm (Figure 4 and Table S2, WT). To our knowledge, this study
260 represents the first observations that clarify the contribution of STT7-dependent LHCII
261 phosphorylation to spillover in green algae.

262   The question arises as to how phospho-LHCIIs contribute to energy migration from PSII
263 to the PSI reaction center. PSII-LHCII supercomplexes, which have phospho-LHCIIs, showed
264 obvious red fluorescence from 700–710 nm (Figures 3 and S6) that were probably due to
265 conformational changes induced by phosphorylation **(31)**. The occurrence of red fluorescence
266 may allow migration of energy from the PSII core to phospho-LHCIIs. Intriguingly, however,
267 delayed fluorescence was also observed in the 709 nm peak region, which represents the
268 fluorescence from LHCIs in the mutant with a deficiency in the PSI core (Figures 4 and S7),
269 suggesting that LHCIs accept energy from PSII-LHCII. Based on these observations, it is
270 possible that an energy-transfer pathway exists between phospho-LHCIIs and LHCIs.

271   Phospho-LHCIIs have been shown to localize around the PsaH subunit in state 2 in a
272 green alga **(32, 33)**, where green algal specific LHCIs (LHCA2 and LHCA9) are predicted to be
273 located **(34, 35)**. The possible interaction between phospho-LHCIIs and LHCA2 and/or LHCA9
274 may contribute to spillover under state 2 conditions. On the other hand, because several LHCIs
275 showed a fluorescence peak near to 709 nm region **(36)**, it was also plausible that those LHCIs
276 (possibly LHCA4, LHCA5, LHCA6, and LHCA8) might contribute to spillover mechanism. Further
277 comprehensive study, including genetic, biochemical, structural, and spectroscopic analyses of
278 the *lhca* mutants, is required to obtain a detailed molecular characterization of the spillover
279 mechanism.

280   Spillover involves a mechanism that uses PSI as a fluorescence quencher to avoid PSII
281 over-excitation **(37)**. Recently, we also discovered light-harvesting complex stress related 1
282 (LHCSR1)-mediated fluorescence quenching in PSI **(38)**. Algae expressing LHCSR1 under
283 ultraviolet radiation showed large fluorescence quenching via increased energy transfer from
284 LHCIIs to PSI. The difference between the spillover and LHCSR1-mediated fluorescence
285 quenching in PSI is defined by pH dependency. The former mechanism does not require a low
286 pH to activate fluorescence quenching, whereas the latter mechanism does. Further, spillover is
287 independent of *de novo* synthesis of quencher proteins such as PsbS, LHCSR1, and LHCSR3.
288 For these reasons, phospho-LHCII-dependent spillover likely serves as a primary acclimatizing
289 response to various environmental conditions. STT7-dependent LHCII phosphorylation is
290 regulated through plastoquinone reduction in response to both light and anoxia **(3)**. The anoxic
291 condition inhibits respiration, which in turn reduces the plastoquinone pool by increasing the total
292 reducing power within cells. Because *Chlamydomonas* species live in soils dominated by
293 bacterial inhabitants **(39)**, algal cells are often exposed to anoxic conditions, particularly during
294 dusk, when photosynthesis is slow. To avoid PSII over-excitation following sunrise, green algae
295 should be able to utilize the phospho-LHCII-dependent spillover system. It is reasonable to
296 expect that the energy redistribution to PSI via spillover could protect PSII, considering that the
297 system is a rapid (assembled without light) and low-cost (no *de novo* protein synthesis required)
298 photoacclimation mechanism. Thus, the spillover system in green algae is likely optimized for
299 survival in native habitats.

300   It appears that spillover is one of several widely conserved photoacclimation mechanisms
301 operating in photosynthetic organisms. Aro and colleagues showed that spillover occurred at the
302 grana margin of the thylakoid membrane in land plants **(15, 16)**. Yokono *et al.* also found the
303 spillover megacomplex in thylakoid membranes from Arabidopsis **(28)**. Here, we discovered
304 phospho-LHCII-mediated spillover in a green alga, whose thylakoid membranes are loosely
305 appressed compared to the grana of land plants **(40)**. The spillover mechanism was also found
306 in red lineages, including a red alga **(28)** and *Symbiodinium* **(41)**. Spillover also occurs in
307 cyanobacteria, which lack chloroplasts and the grana structure of thylakoids **(42-44)**, implying
308 that this mechanism was established at a very primitive stage in the evolution of photosynthesis.
309 Thylakoid membrane structures **(44)** and light-harvesting antennas **(45)** are widely diversified
310 among these photosynthetic organisms: however, it seem that photosynthetic organisms have
311 retained this simple and effective photoprotection mechanism, "spillover", which mainly involves
312 photosystem core complexes, over the course of their evolution.

313

Conclusion

315   The findings of the present study link the conventional molecular mechanism of STT7-
316 dependent state transitions and spillover. In *Chlamydomonas*, phosphorylated LHCIIs mediate
317 facile transfer of energy from PSII-LHCII to PSI-LHCI, which is recognized as spillover. The
318 presence of phospho-LHCII-dependent spillover was first hypothesized over 30 years ago **(30)**;
319 however, this hypothesis was refuted by studies emphasizing phospho-LHCII migration between
320 the photosystems **(13)**. The model presented in this study (Figure 5) overcomes the
321 contradiction between the previous reports because the phospho-LHCIIs mediate both the
322 attachment of LHCII to PSI (state transitions) and direct energy transfer from PSII-LHCII to PSI-
323 LHCI (spillover).

324

Materials and Methods

326 **Culture conditions:** The *C. reinhardtii* strain 137c (mt+) was obtained from the
327 Chlamydomonas Center (http://www.chlamy.org) and was used as the WT strain. The mutant
328 strain *stt7-o* was isolated after performing random mutagenesis. For the random mutagenesis, 1-
329 methyl-3-nitro-1-nitrosoguanidine (Wako, Japan) was used at a final concentration of 5 µg/mL,
330 according to previous reports **(39, 46)**. We screened the mutants, for those were unable to
331 perform qT quenching (state 2 transitions), using a FluoCAM 800MF (Photon System
332 Instruments, Czech Republic). The mutated locus in the *stt7-o* strain was identified by genome
333 sequencing after genetic mapping (Figure S1A), and the obtained *stt7-o* mutant was then
334 backcrossed four times with the WT strain. After the backcross process, we roughly characterize
335 the phenotype through immunoblotting and 77 K fluorescence spectra analysis (Figure S1B-D).
336 The *ΔPSI* (*ΔPsaA*) strain was obtained as described previously **(47)**. All strains were grown in
337 Tris-acetate-phosphate (TAP) medium **(39)** under dim light (< 20 µE m^{-2} s^{-1}) at 23°C until they
338 reached the mid-log growth phase. The culture medium was exchanged with high-salt (HS)
339 minimal medium with slight modifications **(39, 48)** 16 hours before the experiments. In all
340 experiments, the cultured cells were induced to become state 1 with dim far-red light (< 5 µE m^{-2}
341 s^{-1}) at 23°C for 30 min prior to the state 2 induction treatment (dark-anaerobic conditions as
342 previously described **(17)**).

343 **Isolation of thylakoid membranes and photosynthetic supercomplexes:** Thylakoid
344 membranes from the WT and *stt7-o* strains after state 1 or state 2 inductions were isolated as

345 previously reported **(49)**. To purify the photosynthetic supercomplexes from the isolated
346 thylakoids, we used amphipol A8-35, as follows. Thylakoid membranes were detergent-
347 solubilized as described in a previous report **(47)**, then immediately mixed with A8-35 at a final
348 concentration 1.0%, and incubated on ice for 15 minutes. The A8-35-treated membranes were
349 separated by detergent-free sucrose density gradient ultracentrifugation at 230,000 x g for 16
350 hours.

351 **SDS-PAGE and immunoblotting analysis:** SDS-PAGE and immunoblotting analyses were
352 performed as described previously **(50)**. For the phosphorylation analysis, Phospho-Threonine
353 antibody was obtained from Invitrogen (71-8200, rabbit polyclonal), and used as in a previous
354 study **(49)**. Antisera against ATPB was obtained from Agrisera (AS05 085, rabbit polyclonal);
355 antisera against STT7 was raised against synthetic peptide corresponding to 695-713 amino
356 acid of STT7 mature protein. For relative quantification of the phosphorylated proteins, images
357 were analyzed using Image Lab 5.0 software (Bio-Rad, Hercules, CA), and the obtained band
358 intensities were normalized to the intensity of the control samples indicated in the figure legends.

359 **Spectroscopic fluorescence measurements:** Fluorescence quenching kinetics were
360 measured with a PAM-2500 instrument (Walz, Germany) under dark-anaerobic conditions as
361 previously described **(17)**. The functional absorption cross-section that reflects the functional
362 antennae sizes of PSII was measured using a FIRe fluorometer system (Model FIRe; Satlantic,
363 Nova Scotia, Canada), as described previously **(49)**. Low-temperature (77 K) fluorescence
364 spectra were obtained with a FluoroMax4 (HORIBA Jobin-Yvon) as described in a previous
365 study **(51)**. Time-resolved fluorescence decays at room temperature (23°C) were obtained via
366 time-correlated single-photon counting of fluorescence using a FluoroCube (HORIBA Jobin-
367 Yvon) with slight modifications from a previous study **(51)**. A picosecond pulse diode laser (DD-
368 470L; HORIBA Jobin-Yvon) was used to excite chlorophylls at 463 nm with a 10 MHz repetition
369 rate (1.64 pJ/pulse), and emission was detected at 682 nm using a monochromatic detector
370 (bandwidth = 8 nm). To conduct FDAS, time-resolved fluorescence decays at 77 K were
371 obtained by time-correlated single-photon counting of fluorescence as described previously **(28)**.
372 Spectral decomposition was basically performed as described previously **(28)**. In brief, each
373 spectral component is represented as a sum of Gaussian functions. Each spectral component
374 has the same position and width in all samples, and only the amplitude of the spectral
375 components can differ between samples.

376

Acknowledgments

384

Author contributions

386 RT and JM conceived the research. RT designed the experiments, and performed the
387 biochemical and physiological analyses. RT, EK, and SA performed the spectroscopic analysis.
388 EK, SA, MY, and YU analyzed the spectroscopic data. KF-K, and NO isolated the *stt7-o* mutant.

9

389   RT wrote the manuscript with input from all authors. JM supervised the entire research, provided
390   resources, and critically revised the manuscript. All authors contributed to interpretation of the
391   results, and approved the final version of the manuscript.

392

393   **Competing interests**

394   The authors declare no competing interests.

10

395 **References**

396   1.   C. Bonaventura, J. Myers, Fluorescence and oxygen evolution from *Chlorella*
397   *pyrenoidosa. Biochim. Biophys. Acta.* **189**, 366-383 (1969).

398   2.   N. Murata, Control of excitation transfer in photosynthesis I. Light-induced change
399   of chlorophyll *a* fluoresence in *Porphyridium cruentum. Biochim. Biophys. Acta.*
400   **172**, 242-251 (1969).

401   3.   F.-A. Wollman, State transitions reveal the dynamics and flexibility of the
402   photosynthetic apparatus. *EMBO J.* **20**, 3623-3630 (2001).

403   4.   J. Minagawa, State transitions--the molecular remodeling of photosynthetic
404   supercomplexes that controls energy flow in the chloroplast. *Biochim. Biophys.*
405   *Acta.* **1807**, 897-905 (2011).

406   5.   S. Snyders, B. D. Kohorn, Disruption of thylakoid-associated kinase 1 leads to
407   alteration of light harvesting in *Arabidopsis. J. Biol. Chem.* **276**, 32169-32176
408   (2001).

409   6.   N. Depège, S. Bellafiore, J. D. Rochaix, Role of chloroplast protein kinase Stt7 in
410   LHCII phosphorylation and state transition in *Chlamydomonas. Science* **299**,
411   1572-1575 (2003).

412   7.   L. Dumas *et al.*, A stromal region of cytochrome *b6f* subunit IV is involved in the
413   activation of the Stt7 kinase in *Chlamydomonas. Proc. Natl. Acad. Sci. U. S. A.*
414   **114**, 12063-12068 (2017).

415   8.   S. K. Singh *et al.*, Trans-membrane signaling in photosynthetic state transitions:
416   redox- and structure-dependent interaction *in vitro* between STT7 kinase and the
417   cytovhrome *b6f* complex. *J. Biol. Chem.* **291**, 21740-21750 (2016).

418   9.   G. Finazzi, F. Zito, R. P. Barbagallo, F. A. Wollman, Contrasted effects of
419   inhibitors of cytochrome b_6f complex on state transitions in *Chlamydomonas*
420   *reinhardtii*: the role of Qo site occupancy in LHCII kinase activation. *J. Biol. Chem.*
421   **276**, 9770-9774 (2001).

422   10.   S. Lemeille *et al.*, Analysis of the chloroplast protein kinase Stt7 during state
423   transitions. *PLoS Biol.* **7**, e45 (2009).

424   11.   D. J. Kyle, L. A. Staehelin, C. J. Arntzen, Lateral mobility of the light-harvesting
425   complex in chloroplast membranes controls excitation energy distribution in
426   higher plants. *Arch. Biochem. Biophys.* **222**, 527-541 (1983).

427   12.   P. Pesaresi *et al.*, A stable LHCII-PSI aggregate and suppression of
428   photosynthetic state transitions in the *psae1-1* mutant of *Arabidopsis thaliana.*
429   *Planta* **215**, 940-948 (2002).

430   13.   J. F. Allen, J. Forsberg, Molecular recognition in thylakoid structure and function.
431   *Trends Plant Sci.* **6**, 317-326 (2001).

432   14.   S. Zhang, H. V. Scheller, Light-harvesting complex II binds to several small
433   subunits of photosystem I. *J. Biol. Chem.* **279**, 3180-3187 (2004).

434   15.   M. Tikkanen *et al.*, Phosphorylation-dependent regulation of excitation energy
435   distribution between the two photosystems in higher plants. *Biochim. Biophys.*
436   *Acta.* **1777**, 425-432 (2008).

437   16.   M. Grieco, M. Suorsa, A. Jajoo, M. Tikkanen, E. M. Aro, Light-harvesting II
438   antenna trimers connect energetically the entire photosynthetic machinery -
439   including both photosystems II and I. *Biochim. Biophys. Acta.* **1847**, 607-619
440   (2015).

441   17.   W. J. Nawrocki, S. Santabarbara, L. Mosebach, F. A. Wollman, F. Rappaport,
442   State transitions redistribute rather than dissipate energy between the two
443   photosystems in *Chlamydomonas. Nature Plants* **2**, 7 (2016).

11

444 18.   M. Iwai, Y. Takahashi, J. Minagawa, Molecular remodeling of photosystem II
445   during state transitions in *Chlamydomonas reinhardtii*. *Plant Cell* **20**, 2177-2189
446   (2008).
447 19.   M. Iwai, M. Yokono, N. Inada, J. Minagawa, Live-cell imaging of photosystem II
448   antenna dissociation during state transitions. *Proc. Natl. Acad. Sci. U. S. A.* **107**,
449   2337-2342 (2010).
450 20.   C. Ünlü, B. Drop, R. Croce, H. van Amerongen, State transitions in
451   *Chlamydomonas reinhardtii* strongly modulate the functional size of photosystem
452   II but not of photosystem I. *Proc. Natl. Acad. Sci. U. S. A.* **111**, 3460-3465 (2014).
453 21.   A. Watanabe, E. Kim, R. N. Burton-Smith, R. Tokutsu, J. Minagawa, Amphipol-
454   assisted purification method for the highly active and stable photosystem II
455   supercomplex of *Chlamydomonas reinhardtii*. *FEBS Lett.* **593**, 1072-1079 (2019).
456 22.   P. Cardol *et al.*, Impaired respiration discloses the physiological significance of
457   state transitions in *Chlamydomonas*. *Proc. Natl. Acad. Sci. U. S. A.* **106**, 15979-
458   15984 (2009).
459 23.   Z. Liu *et al.*, Crystal structure of spinach major light-harvesting complex at 2.72 A
460   resolution. *Nature* **428**, 287-292 (2004).
461 24.   J. Standfuss, A. C. Terwissscha van Scheltinga, M. Lamborghini, W. Kühlbrandt,
462   Mechanisms of photoprotection and nonphotochemical quenching in pea light-
463   harvesting complex at 2.5 Å resolution. *EMBO J.* **24**, 919-928 (2005).
464 25.   H. Kirchhoff, H. J. Hinz, J. Rosgen, Aggregation and fluorescence quenching of
465   chlorophyll *a* of the light-harvesting complex II from spinach *in vitro*. *Biochim.*
466   *Biophys. Acta.* **1606**, 105-116 (2003).
467 26.   C. Ilioaia, M. P. Johnson, P. Horton, A. V. Ruban, Induction of efficient energy
468   dissipation in the isolated light-harvesting complex of photosystem II in the
469   absence of protein aggregation. *J. Biol. Chem.* **283**, 29505-29512 (2008).
470 27.   M. Mimuro *et al.*, Delayed fluorescence observed in the nanosecond time region
471   at 77 K originates directly from the photosystem II reaction center. *Biochim.*
472   *Biophys. Acta.* **1767**, 327-334 (2007).
473 28.   M. Yokono, A. Takabayashi, S. Akimoto, A. Tanaka, A megacomplex composed
474   of both photosystem reaction centres in higher plants. *Nat. Commun.* **6**, 6 (2015).
475 29.   J. D. Rochaix, Role of thylakoid protein kinases in photosynthetic acclimation.
476   *FEBS Lett.* **581**, 2768-2775 (2007).
477 30.   J. Barber, Influence of surface-charges on thylakoid structure and function. *Annu.*
478   *Rev. Plant Physiol. Plant Mol. Biol.* **33**, 261-295 (1982).
479 31.   H. Zer *et al.*, Regulation of thylakoid protein phosphorylation at the substrate
480   level: Reversible   light-induced   conformational   changes   expose   the
481   phosphorylation site of the light-harvesting complex II. *Proc. Natl. Acad. Sci. U. S.*
482   *A.* **96**, 8277-8282 (1999).
483 32.   Z. H. Huang *et al.*, Structure of photosystem I-LHCI-LHCII from the green alga
484   Chlamydomonas reinhardtii in State 2. *Nat. Commun.* **12** (2021).
485 33.   X. W. Pan *et al.*, Structural basis of LhcbM5-mediated state transitions in green
486   algae. *Nature Plants* **7**, 1119-+ (2021).
487 34.   S.-I. Ozawa *et al.*, Configuration of Ten Light-Harvesting Chlorophyll a/b Complex
488   I Subunits in Chlamydomonas reinhardtii Photosystem I. *Plant Physiol.* **178**, 583-
489   595 (2018).
490 35.   H. Kubota-Kawai *et al.*, Ten antenna proteins are associated with the core in the
491   supramolecular   organization   of   the   photosystem   I   supercomplex   in
492   *Chlamydomonas reinhardtii*. *J. Biol. Chem.* **294**, 4304-4314 (2019).

12

36. M. Mozzo *et al.*, Functional analysis of photosystem I light-harvesting complexes (Lhca) gene products of *Chlamydomonas reinhardtii*. *Biochim. Biophys. Acta.* **1797**, 212-221 (2010).

37. A. Derks, K. Schaven, D. Bruce, Diverse mechanisms for photoprotection in photosynthesis. Dynamic regulation of photosystem II excitation in response to rapid environmental change. *Biochim. Biophys. Acta.* **1847**, 468-485 (2015).

38. K. Kosuge *et al.*, LHCSR1-dependent fluorescence quenching is mediated by excitation energy transfer from LHCII to photosystem I in *Chlamydomonas reinhardtii. Proc. Natl. Acad. Sci. U. S. A.* **115**, 3722-3727 (2018).

39. E. H. Harris, D. B. Stern, G. B. Witman, *The Chlamydomonas Sourcebook 2nd edn*, Academic Press (2009), pp. 1-24.

40. B. D. Engel *et al.*, Native architecture of the Chlamydomonas chloroplast revealed by in situ cryo-electron tomography. *eLife* **4**, 29 (2015).

41. C. Slavov *et al.*, "Super-quenching" state protects Symbiodini*um from ther*mal stress - Implications for coral bleaching. *Biochim. Biophys. Acta.* **1857**, 840-847 (2016).

42. H. J. Liu *et al.*, Phycobilisomes supply excitations to both photosystems in a megacomplex in *Cyanobacteria. Science* **342**, 1104-1107 (2013).

43. S. Akimoto, M. Yokono, E. Yokono, S. Aikawa, A. Kondo, Short-term light adaptation of a cyanobacterium, *Synechocystis* sp. PCC 6803, probed by time-resolved fluorescence spectroscopy. *Plant Physiol. Biochem.* **81**, 149-154 (2014).

44. C. W. Mullineaux, Function and evolution of grana. *Trends Plant Sci.* **10**, 521-525 (2005).

45. A. R. Grossman, D. Bhaya, K. E. Apt, D. M. Kehoe, Light-harvesting complexes in oxygenic photosynthesis: Diversity, control, and evolution. *Annu. Rev. Genet.* **29**, 231-288 (1995).

46. B. Huang, M. R. Rifkin, D. J. L. Luck, Temperature-sensitive mutations affecting flagellar assembly and function in *Chlamydomonas reinhardtii. J. Cell Biol.* **72**, 67-85 (1977).

47. R. Tokutsu, N. Kato, K. H. Bui, T. Ishikawa, J. Minagawa, Revisiting the supramolecular organization of photosystem II in *Chlamydomonas reinhardtii. J. Biol. Chem.* **287**, 31574-31581 (2012).

48. R. Tokutsu, K. Fujimura-Kamada, T. Yamasaki, K. Okajima, J. Minagawa, UV-A/B radiation rapidly activates photoprotective mechanisms in Chlamydomonas reinhardtii. *Plant Physiol.* **185**, 1894-1902 (2021).

49. R. Tokutsu, M. Iwai, J. Minagawa, CP29, a monomeric light-harvesting complex II protein, is essential for state transitions in *Chlamydomonas reinhardtii. J. Biol. Chem.* **284**, 7777-7782 (2009).

50. R. Tokutsu, K. Fujimura-Kamada, T. Matsuo, T. Yamasaki, J. Minagawa, The CONSTANS flowering complex controls the protective response of photosynthesis in the green alga *Chlamydomonas. Nat. Commun.* **10** (2019a).

51. R. Tokutsu, J. Minagawa, Energy-dissipative supercomplex of photosystem II associated with LHCSR3 in *Chlamydomonas reinhardtii. Proc. Natl. Acad. Sci. U. S. A.* **110**, 10016-10021 (2013).

13

538 **Figure legends**
539 **Figure 1. STT7-dependent fluorescence modification under dark-anaerobic conditions.**
540 The WT (blue) and *stt7-o* (red) strains were treated under dark-anaerobic conditions for 20 min.
541 (A) The maximum fluorescence yield, (B) relative PSII antenna absorption cross section, and
542 relative PSI (F713) to PSII (F687) fluorescence signal ratio at low-temperature (77 K) were
543 recorded at the same time points. The ratio was normalized to the initial state (state 1 conditions)
544 of the samples. (D) Phosphorylation of LHCII proteins during the measurements is also shown
545 as a representative example of three biological measurements. n = 3 biological replicates; mean
546 ± s.e.
547
548 **Figure 2. Purification and characterization of PSII-LHCII supercomplexes under state 2**
549 **conditions.**
550 (A) Sucrose gradient fractionation of solubilized state 2 thylakoid membranes. Each band shown
551 is labeled. (B) SDS-PAGE analysis of purified PSII-LHCII supercomplexes from WT and *stt7-o*
552 cells. Sample loading was normalized to 2.5 µg Chl/lane. (C) Immunoblotting analysis performed
553 to visualize phosphorylated polypeptides in the supercomplexes. Phosphorylated proteins were
554 labeled according to SDS-PAGE analysis, as described in a previous study **(47)**. (D) Absorption
555 spectra of the supercomplexes obtained from WT (blue) and *stt7-o* (red) strains normalized at
556 the peak of the Soret region. The spectrum of PSI-LHCI is shown as a control.
557
558 **Figure 3. Time-resolved fluorescence spectra of the isolated PSII-LHCII supercomplexes**
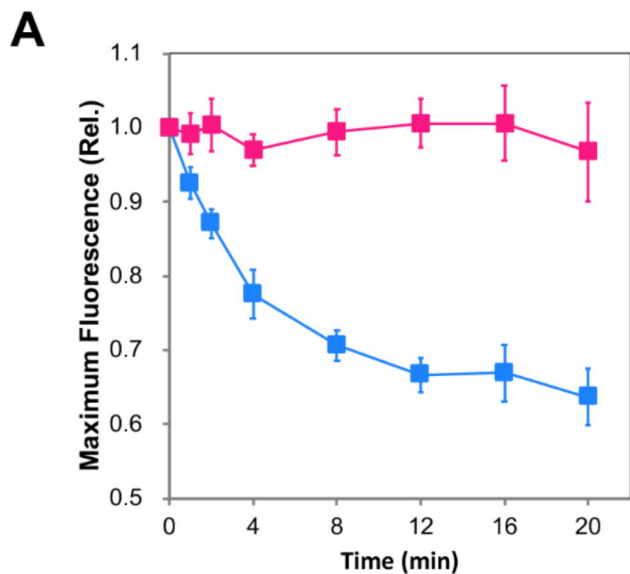559 **and *Chlamydomonas* cells at 77 K.**
560 Time-resolved fluorescence spectra of the PSII-LHCII supercomplexes (gray) were obtained
561 under state 2 conditions from WT (solid line) and *stt7-o* strains (dashed line) at 77 K. WT (blue)
562 and *stt7-o* (red) cells under state 1 (dashed line) and state 2 (solid line) conditions were also
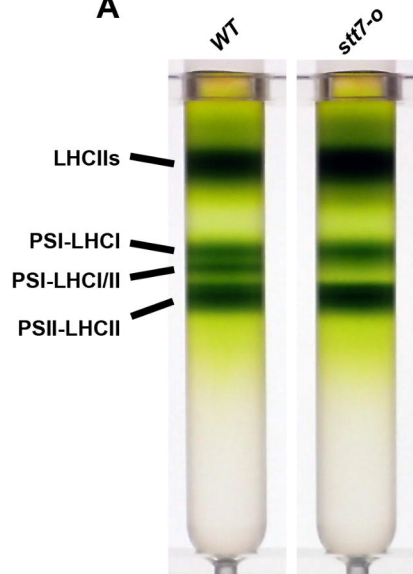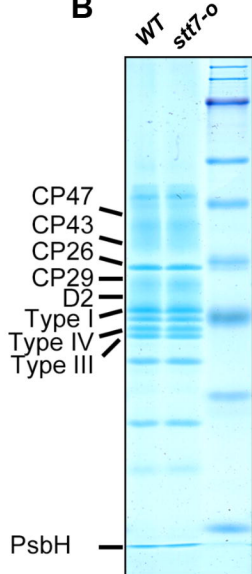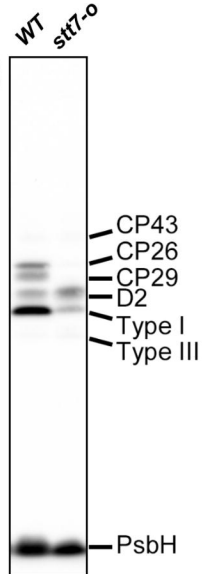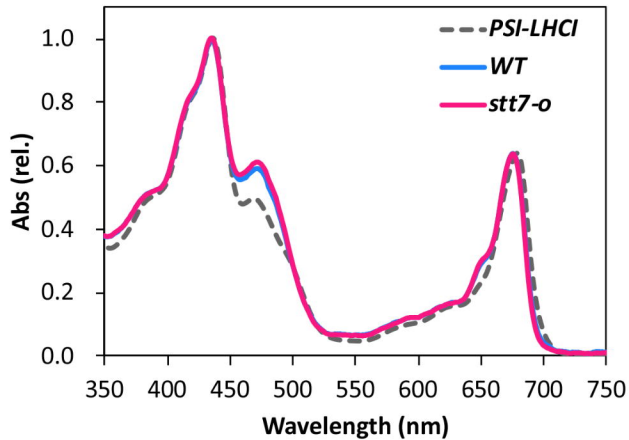563 measured by 459 nm excitation at 77 K.
564
565 **Figure 4. Delayed fluorescence spectra of the isolated PSII-LHCII supercomplexes and**
566 ***Chlamydomonas* cells obtained at 77 K.**
567 FDAS of delayed fluorescence obtained from state 2 PSII-LHCII supercomplexes (Upper; WT,
568 Lower; *stt7-o*,) and cells under state 1 (upper panel) and state 2 (lower panel) conditions were
569 decomposed into six components (details shown in Table 1). Open circles and gray lines
570 represent FDAS spectra and fitting curve, respectively. The peaks and width of components
571 were obtained by global fitting based on wavenumber (cm^{-1}). Each color of component peaks
572 represents 679 nm (cyan, LHCII), 686 nm (blue, CP43), 694 nm (green, CP47), 702 nm (black,
573 phospho-LHCII and/or phospho-PSII), 709 nm (magenta, LHCI) and 717 nm (red, PSI-LHCI).
574 The fluorescence amplitudes were normalized with the total delayed fluorescence intensity of
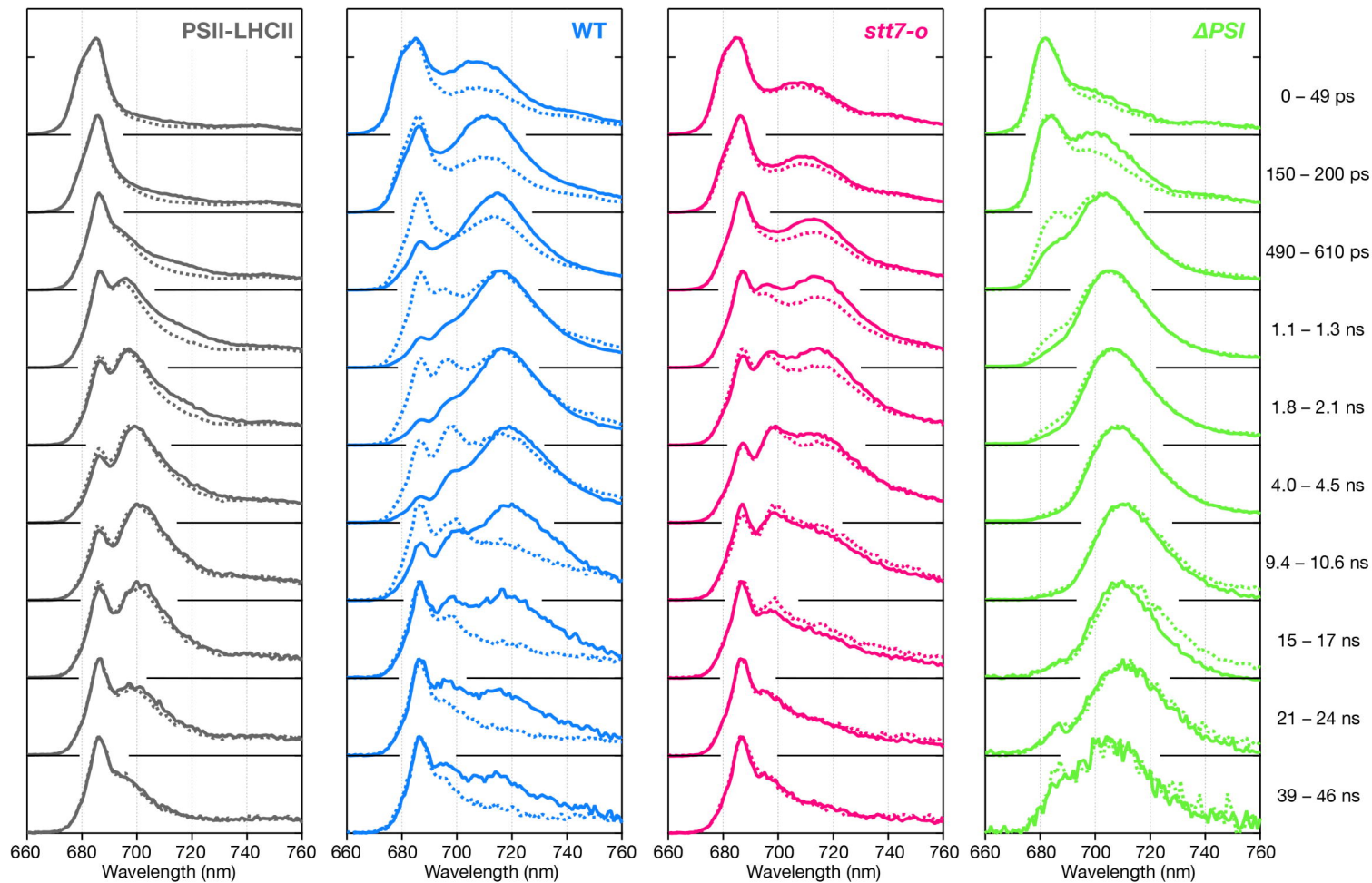575 each samples. Complete FDAS results are shown in Figure S7.
576
577 **Figure 5. Phospho-LHCII regulated spillover between photosystems.**
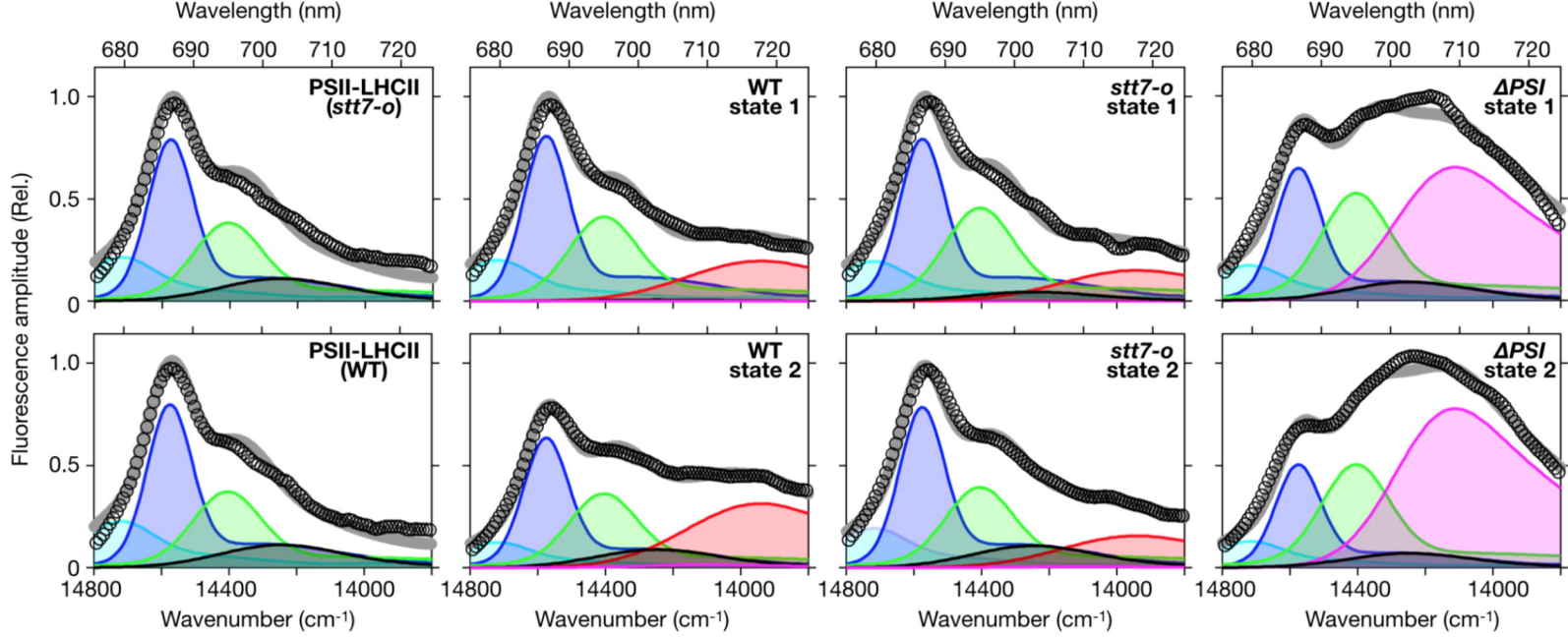578 (A) STT7-dependent phosphorylation under state 2 conditions alters the excitation energy
579 transfer between LHCIIs and PSII. (B) Meanwhile, the PSI-LHCI supercomplex associates with
580 LHCIIs (conventional state 2 transition). (C) The PSI-LHCI(-LHCII) supercomplex approaches
581 the phosphorylated PSII-LHCII supercomplex to form a spillover megacomplex to efficiently
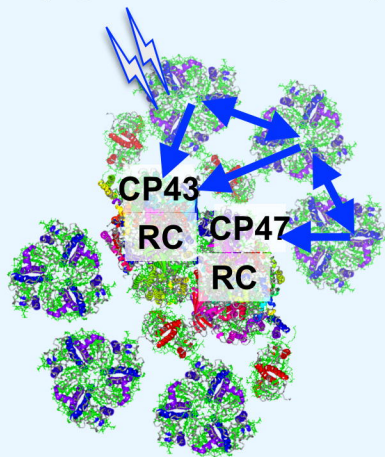582 transfer the excitation energy accumulated in PSII to PSI probably via LHCI.

14

A

B

C

D

min in Dark/Anaerobic

0 1 2 4 8 12 16 20

ATPB

CP26
CP29

LHCII Type I

PSII-LHCII   WT   *stt7-o*   *ΔPSI*

Fluorescence amplitude (rel.)

Wavelength (nm)

0 – 49 ps
150 – 200 ps
490 – 610 ps
1.1 – 1.3 ns
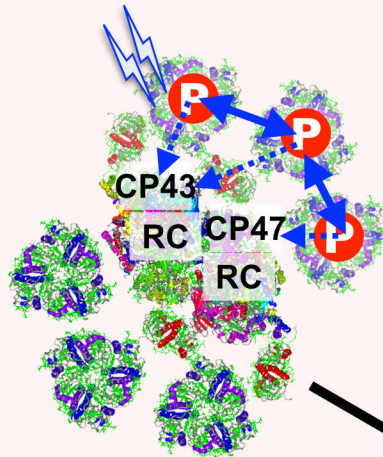1.8 – 2.1 ns
4.0 – 4.5 ns
9.4 – 10.6 ns
15 – 17 ns
21 – 24 ns
39 – 46 ns
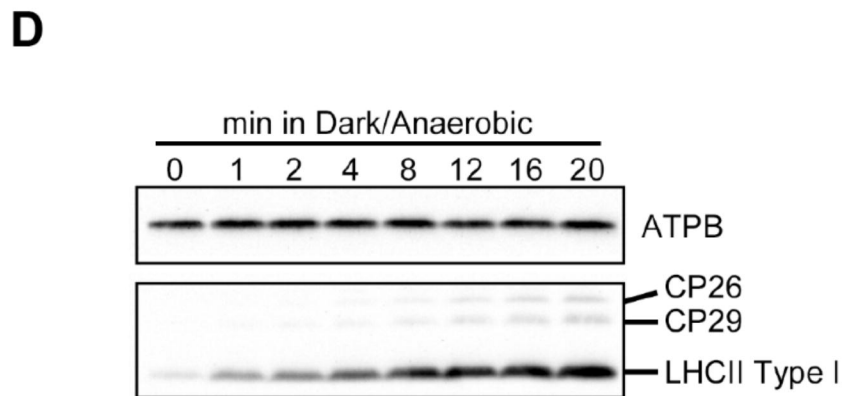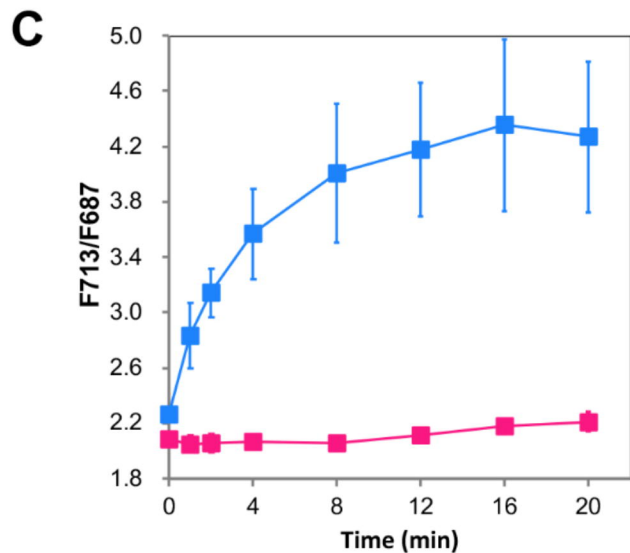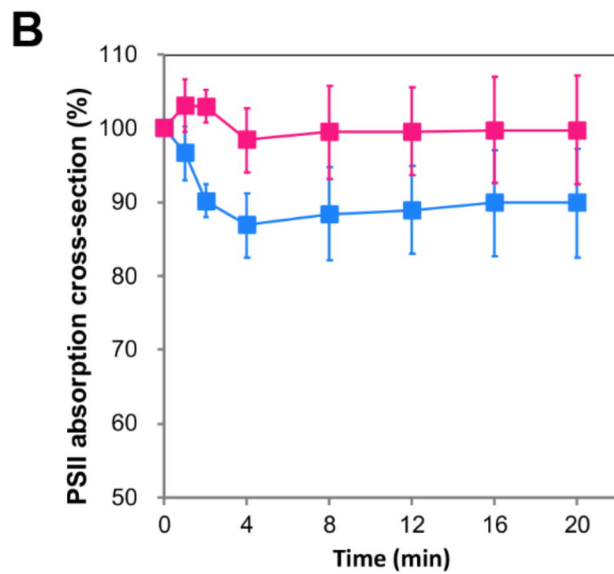
PSII-LHCII
(Light harvesting state)

Phospho-PSII-LHCII
(Altered energy transfer state)

Spill-over megacomplex

CP43

RC

CP47

RC

(A)

PSI-LHCI
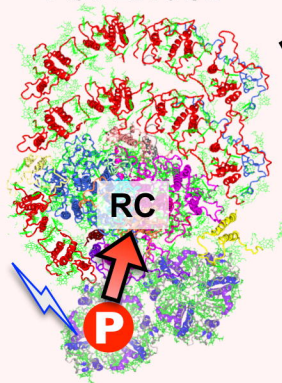
RC

(B)

PSI-LHCI/II

RC

P

(C)

CP43

RC

CP47

RC

P

P

P

RC

P
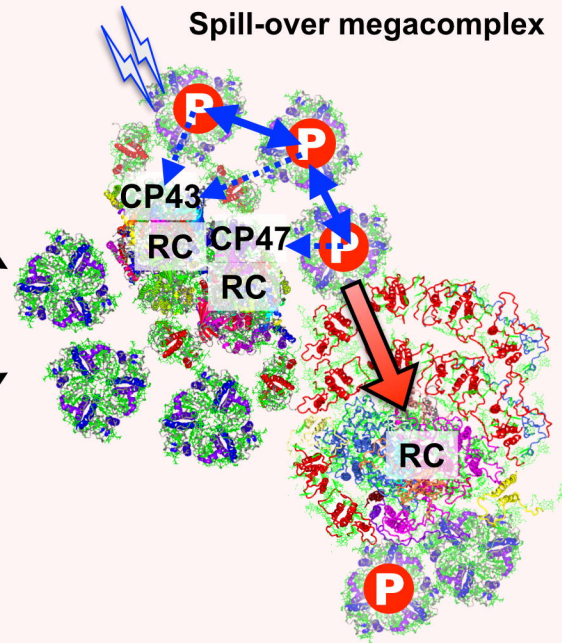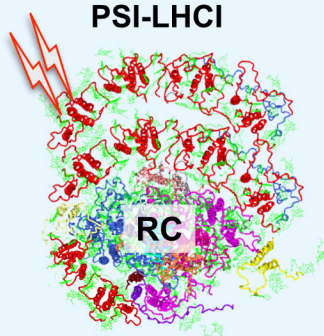
State 1 conditions

State 2 conditions